Available online at www.sciencedirect.com
ScienceDirect
Bioorganic & Medicinal Chemistry 16 (2008) 3482–3488
Bioorganic & Medicinal Chemistry

Structural insights into how irreversible inhibitors can overcome drug resistance in EGFR

Anja Michalczyk, Sabine Klüter, Haridas B. Rode, Jeffrey R. Simard, Christian Grütter, Matthias Rabiller and Daniel Rauh*

Chemical Genomics Centre of the Max-Planck-Society, Otto-Hahn-Strasse 15, 44227 Dortmund, Germany

Received 14 February 2008; accepted 15 February 2008
Available online 20 February 2008

Abstract—Resistance to kinase- targeted cancer drugs has recently been linked to a single point mutation in the ATP binding site of the kinase. In EGFR, the crucial Thr790 gatekeeper residue is mutated to a Met and prevents reversible ATP competitive inhibitors from binding. Irreversible 4-(phenylamino)quinazolines have been shown to overcome this drug resistance and are currently in clinical trials. In order to obtain a detailed structural understanding of how irreversible inhibitors overcome drug resistance, we used Src kinase as a model system for drug resistant EGFR-T790M. We report the first crystal structure of a drug resistant kinase in complex with an irreversible inhibitor. This 4-(phenylamino)quinazoline inhibits wild type and drug resistant EGFR in vitro at low nM concentrations. The co-crystal structure of drug resistant cSrc-T338M kinase domain provides the structural basis of this activity.

1. Introduction

Aberrantly regulated kinases have been shown to play causative roles in diseases such as cancer, diabetes and neurological and autoimmune disorders, making this class of enzymes an important set of therapeutic targets.[1] The tyrosine kinase epidermal growth factor receptor (EGFR) is particularly important since it has been implicated in the development of a variety of human cancers.[2] In addition to EGFR (*erb*B1 (HER1)), activation of all members of the HER receptor family (*erb*B2 (HER2), *erb*B3 (HER3) and *erb*B4 (HER4)) via ligand binding or by point mutations results in cell growth, proliferation, differentiation and migration[3,4] and are associated with more aggressive disease and poorer clinical outcome.[5]

Inspired by the success of Imatinib (Gleevec®; Novartis) as the first targeted cancer therapeutic introduced into the clinic at the start of the millenium for chronic myelogenous leukemia (CML) and gastrointestinal stromal tumour (GISTS),[6,7] a plethora of small organic molecules have since been developed to inhibit kinase function by targeting the ATP binding pocket of the kinase domain.[8–10] 4-(phenylamino)quinazolines such as Erlotinib (Tarceva®; Genentech) and Gefitinib (Iressa®; Astra Zeneca) are a class of potent and selective ATP competitive kinase inhibitors currently available for the treatment of EGFR-associated cancer types. However, a single amino acid mutation (T790M) in the ATP binding pocket of EGFR has been shown to lead to the development of drug resistance and relapse of the disease within months of the initiation of therapy.[11]

The bulkier side chain of the mutated methionine residue is thought to sterically impede binding of these reversible inhibitors and disrupt the formation of a crucial water-mediated hydrogen bond between the inhibitor and T790 of wild type EGFR (Fig. 1).[12]

The T790M mutation in EGFR is structurally analogous to drug resistance mutations in other kinases such as BCR-ABL (T315I), c-KIT (T670I) and platelet-derived growth factor receptor-α (PDGFRα) (T674I)[13] and was predicted to be a hot-spot for drug resistance mutations in EGFR against ATP competitive inhibitors even before the first clinical incidences were reported.[14] More recently, a second class of 4-(phenylamino)quinazolines, which carry a Michael acceptor functional

Keywords: Anticancer agents; Proteins; Crystallography; Drug design; Protein–ligand interactions.
* Corresponding author. E-mail: daniel.rauh@cgc.mpg.de

0968-0896/$ - see front matter © 2008 Elsevier Ltd. All rights reserved.
doi:10.1016/j.bmc.2008.02.053

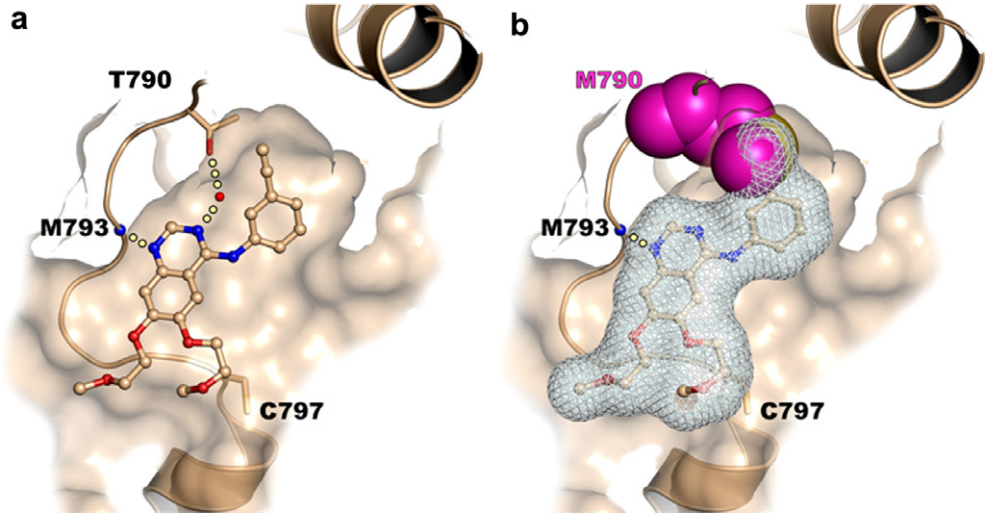

Figure 1. Crystal structure of wild type EGFR complexed with the reversible ATP competitive drug Erlotinib (PDB entry 1M17).[23] (a) Key hydrogen bonds formed between the quinazoline core of the inhibitor and T790 and M793 are indicated by dotted lines. (b) Drug resistance mutation T790M is modelled and displayed in a sphere representation (magenta) and highlights the steric clash with the acetylene moiety of Erlotinib. Van der Waals radii of the inhibitor are shown as mesh surface. Due to the T to M mutation, the water-mediated hydrogen bond between N3 of the quinazoline core and the side chain of T790 is lost.

group at the 6-position and irreversibly alkylate a unique cysteine (C797) in the ATP binding site of EGFR, have been shown to overcome this drug resistance and are currently in phase II/III clinical trials.[15–17] Despite intensive studies, a detailed understanding of how such irreversible inhibitors overcome drug resistance in EGFR-T790M[†] at the atomic level remains limited. In order to address this question, we used organic synthesis, kinetic analysis and protein X-ray crystallography to understand how irreversible inhibitors overcome this mutation-associated drug resistance.

2. Results and discussion

2.1. Chemistry

We synthesized a subset of irreversible 4-(phenylamino)quinazoline-based EGFR inhibitors (**1** and **2**) that vary in the reactivities of their Michael acceptor group (Table 1). Additionally, we synthesized a reversible counterpart of **1**, compound **3**. The synthesis of quinazolines **1**–**3** was done according to published procedures.[18,19] A synthesis scheme and details on compound characterization can be found in the Supplementary Materials. Briefly, N^4-(3-bromophenyl)-4,6-quinazolinediamine was treated with acryloyl chloride and propionyl chloride in the presence of diisopropyl ethyl amine to yield compounds **1** and **3**, respectively. Compound **2** was synthesized from (*E*)-4-(dimethylamino)but-2-enoic acid hydrochloride[18] and N^4-(3-bromophenyl)-4,6-quinazolinediamine (Scheme 1, Supplementary Materials).

[†] During preparation of the manuscript, the crystal structure of the irreversible inhibitor HKI-272 in complex with EGFR-T790M was reported.[33]

Table 1. Inhibition data of compounds **1**–**3** and Erlotinib against EGFR and cSrc mutant variants

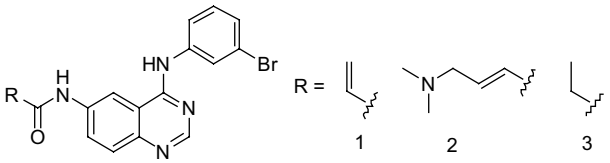

	IC_{50}[a] (nM)			
	1	**2**	**3**	Erlotinib
EGFR	0.08	0.22	0.43	3.6
EGFR-T790M	1.2	3.0	360	260
cSrc-SM	340	236	6400	990
cSrc-DM	2810	5710	>50,000	15,000

[a] Reported values are medians from independent experiments (Supplementary Materials).

2.2. Kinase inhibition

In order to obtain structural information about the binding modes of irreversible inhibitors **1** and **2** to drug resistant kinases, we used the tyrosine kinase cSrc as a model system of EGFR. The kinase domains of EGFR and chicken cSrc share high identity in sequence (37% overall) and structure and the ATP binding sites are highly conserved (70%). We introduced a reactive cysteine (C345) *via* site-directed mutagenesis into a position structurally homologous to C797 in EGFR to create a single mutant cSrc variant (cSrc-SM). This particular cSrc variant has recently been validated as a model system for the structural investigation of irreversible EGFR inhibitors.[20] The high yield bacterial expression of recombinant cSrc,[21] its readiness to crystallize as well as the availability of soaking and co-crystallization systems allows for rapid turnover in the study of protein-ligand

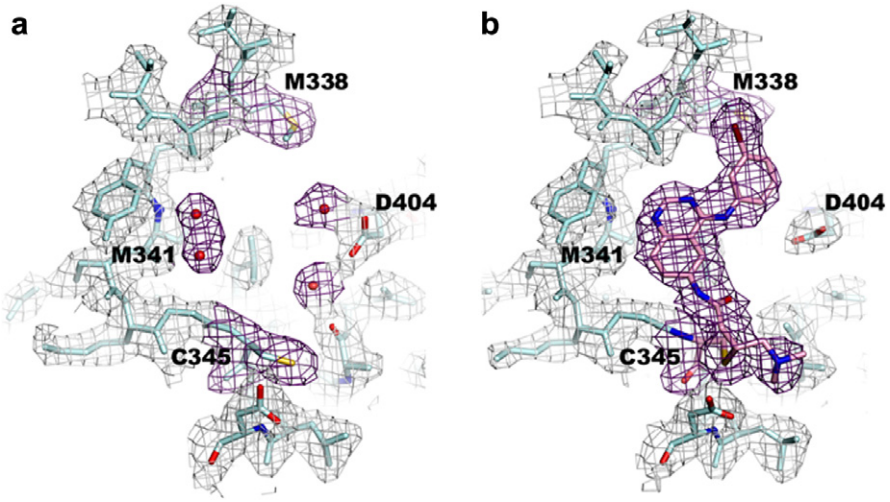

Figure 2. Electron density maps ($2F_o-F_c$ contoured at 1σ) of cSrc-DM in (a) the absence and (b) the presence of **2**.

complexes by X-ray crystallography. Additionally, the cSrc model system is advantageous for the study of homologous protein kinases such as EGFR, which are difficult to handle and often compromised by low diffracting crystals. Similarly, we generated a model system for drug resistant EGFR-T790M by introducing a structurally homologous methionine (M338) to create a drug resistant cSrc double mutant (cSrc-DM). We first performed enzyme activity assays and verified that each cSrc variant was active. Inhibition studies were then performed to demonstrate the different binding specificities of compounds **1**–**3** and Erlotinib in wild type and drug resistant EGFR and cSrc (Table 1).

Although potencies of the inhibitors vary between the tested kinases, the measured IC_{50} values show the expected trend for reversible and irreversible inhibitors. In both EGFR and cSrc, introduction of the drug resistant threonine to methionine mutation causes a decrease in the potency of both reversible (**3**, Erlotinib) and irreversible (**1**, **2**) inhibitors. However, this effect is more pronounced for the reversible inhibitors **3** and Erlotinib. These results are in line with previously published data which showed that irreversible inhibitors overcome mutation-associated drug resistance in EGFR.[13,15,16]

2.3. Structural biology

To gain a deeper structural understanding of how irreversible inhibitors overcome the drug resistance mutation in EGFR-T790M, we determined the crystal structure of apo cSrc-DM (Fig. 2) as well as the structures of **2** co-crystallized with cSrc-SM and cSrc-DM (Fig. 3). Single crystals of the cSrc in complex with **2** were grown in the presence of 1.1-fold molar excess of **2**. From these crystals we could collect X-ray diffraction data to 2.3 Å resolution for cSrc-SM and 2.4 Å resolution for the cSrc-DM. Molecular replacement revealed two molecules in the asymmetric unit, including clear additional electron density at the ligand binding positions. The models were refined to R and R_{free} values of 0.21 and 0.28 for the apo form and 0.21 and 0.27 for the cSrc-SM/DM in complex with **2**, respectively (Table 2).

In the non-ligand bound structure of cSrc-DM, the mutation of T338 into the bulkier and more hydrophobic M338 does not cause major conformational changes within the ATP binding site. However, the side chain conformation of M338 creates a steric impediment that would be expected to interfere with binding of reversible ATP competitive inhibitors such as Erlotinib and **3**, as reflected in our IC_{50} measurements. In the structure of cSrc-SM and cSrc-DM complexed with **2**, the inhibitor adopts binding modes iso-structural to those observed for other irreversible and reversible 4-(phenylamino)quinazolines bound to EGFR and cSrc.[20,22–25] The quinazoline core of **2** is oriented with its N1 forming a key hydrogen bond to the backbone amide NH of M341. Notably, in the presence of **2**, the C^{ε} of M338 is flipped by 180° now pointing towards the back of the ATP binding pocket to avoid the steric clash with the *m*-bromoaniline moiety of the inhibitor (Fig. 3d). The covalent modification of the γ-sulfur of C345 by the electrophile of the inhibitor is clearly indicated by positive difference density and has been confirmed by mass spectroscopy (see Section 4.4 and Supplementary Materials).

3. Conclusions

Application of our structural information gained from cSrc-SM and cSrc-DM in complex with **2** to the problem of drug resistance in EGFR-T790M suggests that a) loss of the water-mediated hydrogen bond between N3 of the quinazoline core and the side chain of wild type T790 of EGFR and b) displacement of C^{ε} of the introduced methionine by the *m*-bromoaniline moiety of the inhibitor to avoid the steric clash, will likely weaken the initial binding interactions for both reversible and irreversible inhibitors, resulting in the observed lower potencies (Table 1). Thus, despite the ability of reversible inhibitors **3** and Erlotinib to inhibit EGFR-T790M at high

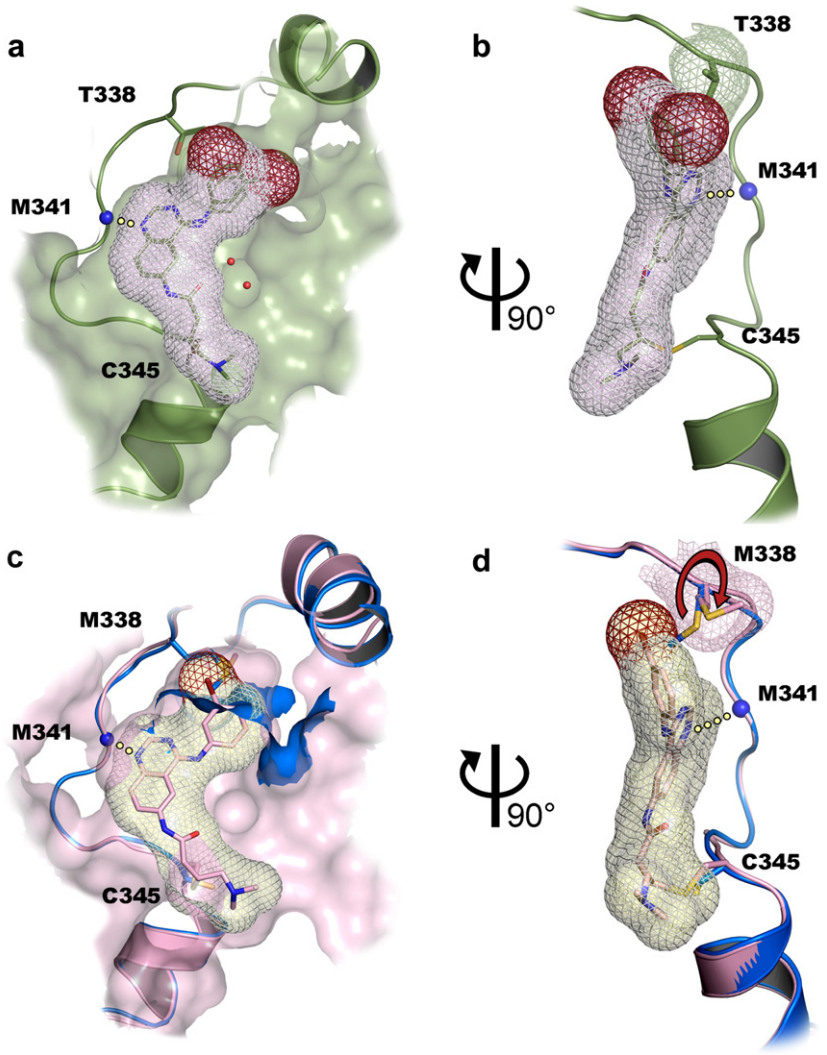

Figure 3. Comparison of the spatial orientation of residues T338 (cSrc-SM, (green)) and M338 (cSrc-DM) in the presence and absence (blue) of **2**. A key hydrogen bond formed between the quinazoline core of the inhibitor and M341 is indicated by a dotted line. (a) Binding of **2** to cSrc-SM. (b) A rotation of about 90° about the *y*-axis reveals the covalent bond formed between **2** and C345 of cSrc-SM. The *m*-bromoaniline moiety of the inhibitor adopts two conformations. (c) Binding of **2** to cSrc-DM induces a conformational change of M338 thereby extending the back of the ATP-binding pocket in order to avoid a steric clash with the *m*-bromoaniline moiety of the inhibitor. (d) A rotation of 90° about the *y*-axis reveals the key interactions between **2** and cSrc-DM and highlights movement of C^{ε} of Met338 (depicted by red arrow). Figures prepared with PyMol.[32]

nanomolar concentrations in vitro, they are unlikely to effectively compete with the high intracellular concentrations of ATP to block EGFR-T790M enzyme activity in cancer cells. In order for irreversible inhibitors to bind, ligand-induced movement of the methionine and formation of the essential hydrogen bond between N1 of the quinazoline and the backbone amide NH of M793 of EGFR must occur to increase the residence time of the inhibitor in the vicinity of the nucleophilic cysteine to result in the Michael addition. In drug resistant EGFR-T790M, these interactions may be partially disrupted. However, the subsequent covalent modification is the event which ultimately shifts the equilibrium between the free and ligand-bound form towards the inactivated state of the kinase, thereby shutting down EGFR enzyme activity.

The use of cSrc as a model system has allowed us to unravel the structural basis by which irreversible 4-(phenylamino)-quinazolines overcome the clinically relevant T790M drug resistance mutation in EGFR. The structural details gained from our studies show that the side chain of the mutant methionine gatekeeper interacts with both, reversible and irreversible 4-(phenylamino)-quinazoline-based EGFR inhibitors and interferes with ligand binding. Our results should prove useful for the design of kinase inhibitors that account for the prominent problem of drug resistance in kinase-targeted cancer therapy.

4. Experimental

Anhydrous solvents were purchased from Acros Organics and Fluka. Other chemical materials were purchased from Alfa Aesar, Fluka and Sigma Aldrich and were used as received. Site-directed mutagenesis of cSrc was performed using a standard site-directed mutagenesis

Table 2. Statistics for data collection and refinement of apo cSrc-DM, cSrc-SM/DM + **2**

Data collection	cSrc-SM + **2**	cSrc-DM	cSrc-DM + **2**
Space group	*P*1	*P*1	*P*1
Resolution (Å)	2.33–72.94	2.32–72.55	2.38–73.57
Highest Shell (Å)	2.33–2.46	2.32–2.45	2.38–2.51
Cell dimensions			
a, *b*, *c* (Å)	41.94; 63.53; 74.50	42.00; 63.02; 73.95	42.22; 63.36; 75.06
α, β, γ (Å)	78.28; 90.37; 89.45	78.78; 88.80; 90.14	78.58; 89.08; 89.87
R_{sym}	6.0 (40.7)	7.5 (37.0)	6.9 (12.6)
Unique reflections	29165	30188	29935
Completeness (%)	90.7 (85.9)	93.8 (91.2)	98.0 (96.9)
Average redundancy	3.6	2.2	2.1
Refinement			
R_{work}/R_{free}	21.2/26.7	20.5/28.0	21.4/26.6
No. of atoms			
Protein A,B	1923, 1970	2049, 1983	1988, 1950
Ligand A, B	54, 27	No ligand	27, 27
Water	99	172	168
Average B-factors (Å^2)			
Protein A, B	32.1, 32.7	34.4, 34.0	33.7, 33.6
Ligand A, B	39.5, 62.5	No ligand	64.9, 59.9
Water	27.2	28.6	29.9
R.m.s. deviations			
Bond lengths (Å)	0.016	0.016	0.018
Angles (°)	1.770	1.782	1.841
Ramachandran outliers (%)	0	0	0
PDB accession code	2QLQ	2QI8	2QQ7

kit (Qiagen). Enzyme kinetics were measured using a commercial FRET-based assay system (Z'lyte^{TM}) available from Invitrogen (#PV3191 and #PV3193). Wild type EGFR was purchased from Invitrogen (#PV3872) and EGFR-T790M was purchased from Upstate (# 14–725).

4.1. Synthesis of compounds

All 4-(phenylamino)quinazolines were prepared according to the literature procedures (Supplementary Material). ^{1}H and ^{13}C NMR spectra were recorded on a Varian Mercury 400, Bruker DRX 500 or Varian Inova 600 spectrometer using dimethylsulfoxide-d_6 as an internal reference. Chemical shifts (δ) are given in ppm and coupling constants (*J*) were measured in Hz. The following abbreviations are used; s-singlet, d-doublet, dd-doublet of doublet, t-triplet, td-triplet of doublet, q-quartet, qd-quartet of doublet, br-broad. LC–MS spectra were obtained on a LTQ Orbitrap (high resolution mass spectrometer from Thermo Electron) coupled to an 'Accela' HPLC System (consisting of Accela pump, Accela autosampler and Accela PDA detector) supplied with a 'Hypersil GOLD' column (50 mm × 1 mm, 1.9 μm particle size) from Thermo Electron. Melting points were determined using open glass capillaries on a Büchi melting point apparatus (B-540) and are uncorrected. Analytical TLC was carried out on Merck 60 F_{245} aluminium-backed silica gel plates. Compounds were purified by column chromatography using Baker silica gel (40–70 μm particle size). Preparative HPLC was carried out on the final compounds using a Varian Prostar with UV-detector (Model 340) and a VP 25-21 Nucleodur (C18 Gravity, 5 μ) column (Serial no. 2105150).

4.2. Protein expression and purification

Prior to expression, mutations of T338 to methionine and S345 to cysteine were introduced by site-directed mutagenesis and confirmed by sequence analysis. The T338M mutation was introduced using the following primer sequences: 5′-AGCCCATCTACATCGTCATG GAGTACATGAGCAAGGGG-3′ and 5′-CCCCTTG CTCATGTACTCCATGACGATGTAGATGGGCT-3′. The S345C mutation was introduced using the following primer sequences: 5′-GTACATGAGCAAGGGGGTC TGCCTCCTGGATTTCCTG-3′ and 5′-CAGGAAA TCCAGGAGGCAGACCCCCTTGCTCATGTAC-3′. All chicken cSrc (residues 251–533) variants were co-expressed in *E. coli* and purified as previously described.[20,21]

4.3. IC_{50} determination

IC_{50} values were determined with the Z'lyte^{TM} assay system. The reactions were performed with a 10 μl total volume in 384-well small volume plates from Greiner (#784076). The kinase reaction for cSrc consisted of kinase buffer (50 mM HEPES pH 7.5, 0.01% BRIJ-35, 10 mM $MgCl_2$, 1 mM EGTA), 1–15 nM kinase, 2 μM peptide and either 25 μM ATP for cSrc-SM or 15 μM ATP for cSrc-DM. For each IC_{50} determination, 16 different concentrations of inhibitor (range from 250,000 to 10 nM) were used in triplicate and at least three inde-

pendent experiments were performed. Before starting the kinase reaction, enzyme and inhibitor were incubated for 40 min. The kinase reaction for EGFR consisted of BSA-supplemented kinase buffer (25 mM HEPES pH 7.5, 0.005% BRIJ-35, 2 mM $MnCl_2$, 10 mM $MgCl_2$, 1 mM DTT, 2.5 mM $CaCl_2$ and 0.1 mg/ml BSA), 1–5 nM kinase, 0.5 μM peptide, 7 μM ATP for wild type EGFR and 2 μM ATP for EGFR-T790M. For IC_{50} determinations, 10 different concentrations (ranging from 0.1 nM to 10 μM) of inhibitor were used in duplicate. Each experiment was repeated at least twice. Following the kinase reaction, 5 μl of Development Solution (included with the kit) was added to cleave the remaining unphosphorylated peptide. Following a 1 h incubation time with Development Solution, 5 μl of Stop Solution (included with the kit) was added to the reaction mixture to bring the final volume to 20 μl. Fluorescence was then measured with a Spectramax® M5 plate reader from Molecular Devices (cSrc experiments) or a Safire^{2TM} from Tecan. Upon excitation of coumarin at 400 nm, fluorescence emission was measured at 445 nm (coumarin) and 520 nm (fluorescein). The ratio of coumarin to fluorescein emission ($R = \lambda 445/\lambda 520$) was used to calculate the percentage of phosphorylation of the peptide by the kinase.

4.4. Mass spectroscopy experiments

Mass spectroscopy analysis was carried out by first incubating cSrc-DM (12.5 μM) with an equimolar amount of each irreversible inhibitor for 40 min at RT. After dialyzing against deionized water, the protein-inhibitor complex was prepared for analysis by mixing 4 μl of the dialyzed protein with 16 μl deionized water and 20 μl of an acetonitrile/formic acid (2% v/v) solution. Aliquots (20 μl) were analyzed by ESI-MS using a Finnigan LCQ Advantage Max mass spectrometer from Thermo. Deconvolution and visualization were performed using the BioWorks 3.1 (SR_1) from Thermo Scientific.

4.5. Crystallization

Crystals of suitable size were grown by vapour diffusion (using the hanging-drop method) at 298 K against well solutions containing 15–20% (w/v) ethylene glycol. For co-crystallization experiments, preincubations were carried out with a ratio of 1:1.1 protein to inhibitor (10 mM in DMSO). Plate-like crystals of the triclinic space group P1 were obtained after one week.

4.6. Data collection and refinement

Datasets for apo cSrc-DM and cSrc-SM complexed with **2** were measured in-house (Rigaku MicroMax-007, MPI Dortmund). A dataset of cSrc-DM in complex with **2** was measured at the X10SA beamline of the Swiss Light Source (PSI, Villingen, Switzerland). Datasets were integrated using MOSFLM and scaled with SCALA (CCP4[26] package 5.0.2). The structures were solved by molecular replacement with PHASER.[27] Starting coordinates were taken from cSrc-SM in complex with **1** (PDB accession code 2HWP[20]). Crystallographic refinement and electron density maps calculation were carried out using REFMAC5.[28] Compound **2** was constructed and minimized with DS ViewerPro 6.0 (Accelrys Software Inc.). Topology files were generated using the Dundee PRODRG2[29] server. Model building was done using COOT.[30] Detailed data and refinement statistics are given in Table 2. Atomic coordinates for apo cSrc-DM and cSrc-DM-**2** and cSrc-SM-**2** complex structures have been deposited to the Protein Data Bank (Accession codes 2QI8, 2QQ7 and 2QLQ). Refined structures were validated with PROCHECK.[31] Figures were produced using PyMol 2002 (DeLano Scientific, San Carlos, CA, USA).

Acknowledgment

J.R.S. was funded by the Alexander von Humboldt Foundation. Organon/Schering Plough, Bayer-Schering Pharma, Merck-Serono and BayerCrop Science are thanked for financial support. We thank Roman Thomas for Erlotinib.

Supplementary data

Supplementary data associated with the chemical synthesis of 4-(phenylamino)quinazolines and ESI-MS analysis can be found online. Supplementary data associated with this article can be found, in the online version, at doi:10.1016/j.bmc.2008.02.053.

References and notes

1. Gschwind, A.; Fischer, O. M.; Ullrich, A. *Nat. Rev. Cancer* **2004**, *4*, 361–370.
2. Schlessinger, J. *Science* **2004**, *306*, 1506–1507.
3. Arteaga, C. L. *J. Clin. Oncol.* **2001**, *19*, 32S–40S.
4. Dowell, J. E.; Minna, J. D. *Nat. Clin. Pract. Oncol.* **2004**, *1*, 2–3.
5. Temam, S.; Kawaguchi, H.; El-Naggar, A. K.; Jelinek, J.; Tang, H.; Liu, D. D.; Lang, W.; Issa, J. P.; Lee, J. J.; Mao, L. *J. Clin. Oncol.* **2007**, *25*, 2164–2170.
6. Holtz, M. S.; Slovak, M. L.; Zhang, F.; Sawyers, C. L.; Forman, S. J.; Bhatia, R. *Blood* **2002**, *99*, 3792–3800.
7. Zhang, P.; Gao, W. Y.; Turner, S.; Ducatman, B. S. *Mol. Cancer* **2003**, *2*, 1.
8. Baselga, J.; Arteaga, C. L. *J. Clin. Oncol.* **2005**, *23*, 2445–2459.
9. El-Obeid, A.; Hesselager, G.; Westermark, B.; Nister, M. *Biochem. Biophys. Res. Commun.* **2002**, *290*, 349–358.
10. Hynes, N. E.; Lane, H. A. *Nat. Rev. Cancer* **2005**, *5*, 341–354.
11. Sharma, S. V.; Bell, D. W.; Settleman, J.; Haber, D. A. *Nat. Rev. Cancer* **2007**, *7*, 169–181.
12. Kobayashi, S.; Boggon, T. J.; Dayaram, T.; Janne, P. A.; Kocher, O.; Meyerson, M.; Johnson, B. E.; Eck, M. J.; Tenen, D. G.; Halmos, B. *N. Engl. J. Med.* **2005**, *352*, 786–792.
13. Carter, T. A.; Wodicka, L. M.; Shah, N. P.; Velasco, A. M.; Fabian, M. A.; Treiber, D. K.; Milanov, Z. V.; Atteridge, C. E.; Biggs, W. H., 3rd; Edeen, P. T.; Floyd, M.; Ford, J. M.; Grotzfeld, R. M.; Herrgard, S.; Insko, D. E.; Mehta, S. A.; Patel, H. K.; Pao, W.; Sawyers, C. L.;

Varmus, H.; Zarrinkar, P. P.; Lockhart, D. J. *Proc. Natl. Acad. Sci. U.S.A.* **2005**, *102*, 11011–11016.
14. Blencke, S.; Ullrich, A.; Daub, H. *J. Biol. Chem.* **2003**, *278*, 15435–15440.
15. Kobayashi, S.; Ji, H.; Yuza, Y.; Meyerson, M.; Wong, K. K.; Tenen, D. G.; Halmos, B. *Cancer Res.* **2005**, *65*, 7096–7101.
16. Kwak, E. L.; Sordella, R.; Bell, D. W.; Godin-Heymann, N.; Okimoto, R. A.; Brannigan, B. W.; Harris, P. L.; Driscoll, D. R.; Fidias, P.; Lynch, T. J.; Rabindran, S. K.; McGinnis, J. P.; Wissner, A.; Sharma, S. V.; Isselbacher, K. J.; Settleman, J.; Haber, D. A. *Proc. Natl. Acad. Sci. U.S.A.* **2005**, *102*, 7665–7670.
17. Pao, W.; Miller, V. A.; Politi, K. A.; Riely, G. J.; Somwar, R.; Zakowski, M. F.; Kris, M. G.; Varmus, H. *PLoS Med.* **2005**, *2*, e73.
18. Considine, J. L.; Daigneault, S.; Chew, W.; Iera, S.; Duncan, S. M.; Ren, J. World Patent 2004066919, CAN 141:17382, 2004.
19. Tsou, H. R.; Mamuya, N.; Johnson, B. D.; Reich, M. F.; Gruber, B. C.; Ye, F.; Nilakantan, R.; Shen, R.; Discafani, C.; DeBlanc, R.; Davis, R.; Koehn, F. E.; Greenberger, L. M.; Wang, Y. F.; Wissner, A. *J. Med. Chem.* **2001**, *44*, 2719–2734.
20. Blair, J. A.; Rauh, D.; Kung, C.; Yun, C. H.; Fan, Q. W.; Rode, H.; Zhang, C.; Eck, M. J.; Weiss, W. A.; Shokat, K. M. *Nat. Chem. Biol.* **2007**, *3*, 229–238.
21. Seeliger, M. A.; Young, M.; Henderson, M. N.; Pellicena, P.; King, D. S.; Falick, A. M.; Kuriyan, J. *Protein Sci.* **2005**, *14*, 3135–3139.
22. Hennequin, L. F.; Allen, J.; Breed, J.; Curwen, J.; Fennell, M.; Green, T. P.; Lambert-van der Brempt, C.; Morgentin, R.; Norman, R. A.; Olivier, A.; Otterbein, L.; Ple, P. A.; Warin, N.; Costello, G. *J. Med. Chem.* **2006**, *49*, 6465–6488.
23. Stamos, J.; Sliwkowski, M. X.; Eigenbrot, C. *J. Biol. Chem.* **2002**, *277*, 46265–46272.
24. Wood, E. R.; Truesdale, A. T.; McDonald, O. B.; Yuan, D.; Hassell, A.; Dickerson, S. H.; Ellis, B.; Pennisi, C.; Horne, E.; Lackey, K.; Alligood, K. J.; Rusnak, D. W.; Gilmer, T. M.; Shewchuk, L. *Cancer Res.* **2004**, *64*, 6652–6659.
25. Yun, C. H.; Boggon, T. J.; Li, Y.; Woo, M. S.; Greulich, H.; Meyerson, M.; Eck, M. J. *Cancer Cell* **2007**, *11*, 217–227.
26. Collaborative Computational Project, N. *Acta Crystallogr. D* **1994**, *50*, 760–763.
27. Read, R. J. *Acta Crystallogr. D* **2001**, *57*, 1373–1382.
28. Murshudov, G. N.; Vagin, A. A.; Dodson, E. J. *Acta Crystallogr. D* **1997**, *53*, 231–354.
29. Schüttelkopf, A. W.; Aalten, D. M. F. v. *Acta Crystallogr. D* **2004**, *60*, 1355–1363.
30. Emsley, P.; Cowtan, K. *Acta Crystallogr. D* **2004**, *60*, 2126–2132.
31. Laskowski, R. A.; MacArthur, M. W.; Moss, D. S.; Thornton, J. M. *J. Appl. Crystallogr.* **1993**, *26*, 283–291.
32. DeLano, W. L. http://www.pymol.org bf 2002.
33. Yun, C. H.; Mengwasser, K. E.; Toms, A. V.; Woo, M. S.; Greulich, H.; Wong, K. K.; Meyerson, M.; Eck, M. J. *Proc. Natl. Acad. Sci. U.S.A.* **2008**.